JOURNAL OF AGRICULTURAL AND FOOD CHEMISTRY

ARTICLE

pubs.acs.org/JAFC

Molecular Spectroscopic Studies of Farrerol Interaction with Calf Thymus DNA

Guowen Zhang,* Peng Fu, Lin Wang, and Mingming Hu

State Key Laboratory of Food Science and Technology, Nanchang University, 235 Nanjing East Road, Nanchang 330047, China

ABSTRACT: The interaction between farrerol and calf thymus DNA in a pH 7.4 Tris-HCl buffer was investigated with the use of neutral red (NR) dye as a spectral probe by UV−vis absorption, fluorescence, and circular dichroism (CD) spectroscopy, as well as viscosity measurements and DNA melting techniques. It was found that farrerol molecules could intercalate into the base pairs of DNA as evidenced by decreases in iodide quenching effect and single-stranded DNA (ssDNA) quenching effect, induced CD spectral changes, and significant increases in relative viscosity and denaturation temperature of DNA. Furthermore, the spectral data matrix of the competitive reaction between farrerol and NR with DNA was resolved with an alternative least-squares (ALS) algorithm, and the concentration profiles in the reaction and the corresponding pure spectra for three species (farrerol, NR, and DNA−NR complex) were obtained. This ALS analysis demonstrated the intercalation of farrerol to the DNA by substituting for NR in the DNA−NR complex. Moreover, the thermodynamic parameters enthalpy change ($\Delta H°$) and entropy change ($\Delta S°$) were calculated to be -16.49 ± 0.51 kJ mol^{-1} and 32.47 ± 1.02 J mol^{-1} K^{-1} via the van't Hoff equation, which suggested that the binding of farrerol to DNA was driven mainly by hydrophobic interactions and hydrogen bonds.

KEYWORDS: farrerol, calf thymus DNA, binding mode, spectroscopy, alternative least-squares

INTRODUCTION

DNA is quite often the main cellular target for studies with small molecules of biological importance such as carcinogens, steroids, and several classes of drugs.[1] There is growing interest in exploring the binding of small molecules with DNA for the rational design and construction of new and more efficient drugs targeted to DNA.[2] Generally, there are three modes for binding of small molecules with double-helix DNA in a noncovalent way: (i) electrostatic interaction, electrostatic attractions with the anionic sugar−phosphate backbone of DNA; (ii) groove binding, interactions with the DNA groove; and (iii) intercalation between the base pairs.[3] Intercalative binding and groove binding are related to the grooves in the DNA double helix, but the electrostatic binding can take place out of the groove. Among the three modes, the most effective mode of the drugs targeted to DNA is intercalative binding, which is related to the antitumor activity of the compound.[4]

Flavonoids are a large group of polyphenolic natural products that are widely distributed in fruits, vegetables, nuts, and beverages.[5−7] They have been reported to exhibit several health beneficial effects by acting as antioxidant, anticarcinogen, cardiopreventive, antimicrobial, antiviral, antiallergic, and neuroprotective agents.[8,9] Farrerol (structure shown in Figure 1), a flavonoid compound, is the main active component of *Rhododendron dauricum* L., which is one natural plant used as a traditional Chinese herbal medicine.[10] Investigations have shown that farrerol has a wide range of biological and pharmacological activities, including anti-inflammatory, antibacterial, and antioxidant activities and inhibition of a variety of enzymes.[11,12] Shi et al.[13] reported that farrerol has good in vitro antitumor activity against SGC-7901 cells in a time- and dose-dependent manner. However, to our knowledge, the mechanism of interaction between farrerol and DNA has not been previously reported.

Some techniques are commonly used to detect the interaction between DNA and small molecules, including fluorescence spectroscopy,[14] UV spectrophotometry,[15] circular dichroism (CD),[16] Fourier transform infrared (FT-IR) spectroscopy,[17] nuclear magnetic resonance (NMR),[18] and electrospray ionization mass spectrometry (EI-MS).[19] Among these techniques, UV−vis absorption and fluorescence spectroscopy are well-known and employed as simple but sensitive methods. In recent years, the application of chemometrics methods in the life sciences has drawn much attention, because they can provide information well beyond that obtained by conventional methods. Alternate least-squares (ALS) is a well-known soft modeling algorithm,[20] which has been applied for analyses of spectroscopic and electrochemical data from biomolecular equilibria in solution, and the equilibrium concentration of each component in the reaction as well as the corresponding pure spectra were obtained simultaneously.[21−23]

In the present study, the interaction of farrerol (Figure 1) with calf thymus DNA was investigated in vitro using neutral red (NR) dye as a spectral probe by the application of UV−vis absorption, fluorescence, and CD spectroscopy, as well as viscosity measurements and DNA melting techniques. The binding mode of farrerol to DNA was estimated. Furthermore, a chemometrics approach, the ALS algorithm, was used to verify the binding mode between farrerol and DNA by resolving the overlapping UV−vis absorption spectra of competitive reaction of farrerol and NR with DNA. The equilibrium concentration profiles of each component in the reaction and the corresponding pure spectra were extracted satisfactorily. It should be noted that such

Received: May 13, 2011
Revised: July 12, 2011
Accepted: July 16, 2011
Published: July 16, 2011

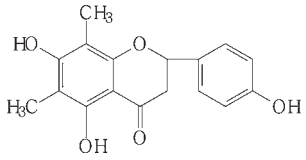

Figure 1. Structure of farrerol.

extracted information is unobtainable with the use of conventional methods of data interpretation. We hope that this work can benefit further understanding of the binding mechanism of farrerol with DNA and comprehension farrerol's pharmacological effects as well as the design of the structure of new and efficient drug molecules.

MATERIALS AND METHODS

Instrumentations. Fluorescence measurements were performed with a Hitachi spectrofluorometer model F-4500 equipped with a 150 W xenon lamp and a thermostat bath, using a 1.0 cm quartz cell. The widths of both the excitation slit and emission slit were set at 5.0 nm. The absorption spectra were measured on a Shimadzu UV-2450 spectrophotometer using a 1.0 cm cell. The CD spectra were recorded on a Bio-Logic MOS 450 CD spectrometer (France) using a 1.0 mm path length quartz cuvette. pH measurements were taken with a pHS-3C digital pH-meter (Shanghai Exact Sciences Instrument Co. Ltd., Shanghai, China) with a combined glass−calomel electrode. The viscosity measurements were performed on an NDJ-79 viscosity meter (Yinhua Flowmeter Co. Ltd., Hangzhou, China). An electronic thermostat water bath (Shanghai Yuejin Medical Instrument Co., Shanghai, China) was used for controlling the temperature.

Chemicals and Reagents. Farrerol (analytical grade) was obtained from the National Institute for the Control of Pharmaceutical Biological Products (Beijing, China). The stock solution (3.40×10^{-3} mol L^{-1}) of farrerol was prepared in absolute methanol. Calf thymus DNA (Sigma Chemical Co., St. Louis, MO) was used without further purification, and its stock solution was prepared by dissolving an appropriate amount of DNA in doubly distilled water. Then the solution was allowed to stand overnight and stored at 4 °C in the dark for about a week. The concentration of DNA in stock solution was determined to be 2.66×10^{-3} mol L^{-1} by UV absorption at 260 nm using a molar absorption coefficient $\varepsilon_{260} = 6600$ L mol^{-1} cm^{-1} (expressed as molarity of phosphate groups).[24] The purity of the DNA was checked by monitoring the ratio of the absorbance at 260 nm to that at 280 nm. The solution gave a ratio of >1.8 at A_{260}/A_{280}, which indicates that DNA was sufficiently free from protein.[25] NR stock solution (2.0×10^{-3} mol L^{-1}) was prepared by dissolving its crystals (Sigma Chemical Co.) in doubly distilled water and storing it in a cool and dark place. All of the solutions were adjusted with Tris-HCl buffer solution (0.05 mol L^{-1}, pH 7.4), which was prepared by mixing and diluting 25 mL of Tris solution (0.2 mol L^{-1}) with 45 mL of HCl (0.1 mol L^{-1}) and then diluting it to 100 mL. All chemicals were of analytical reagent grade, and doubly distilled water was used throughout.

Resonance Light Scattering (RLS) Spectra. An appropriate aliquot of DNA solutions was added to a fixed volume of farrerol solution and diluted to 10 mL with the Tris-HCl buffer solution (pH 7.4). RLS spectra were obtained by synchronous scanning on the spectrofluorometer with the wavelength range of 200−700 nm at room temperature. The widths of both the excitation slit and emission slit were set at 10 nm.

UV−Vis Measurements. The UV−vis absorption spectra of farrerol and the mixture of DNA and farrerol were measured in the wavelength range of 220−370 nm.

The competitive interaction between farrerol and NR dye with DNA was performed as follows: fixed amounts of NR and DNA were titrated with increasing amounts of farrerol solution. After these solutions had been allowed to stand for 8 min to equilibrate, the UV−vis measurements were then made. All UV−vis measurements were carried out in 0.05 mol L^{-1} Tris-HCl buffer (pH 7.4) at room temperature.

Fluorescence Measurements. A 3.0 mL solution, containing 5.1×10^{-5} mol L^{-1} farrerol, was titrated by successive additions of DNA (to give a final concentration of 6.91×10^{-5} mol L^{-1}). These solutions were allowed to stand for 8 min to equilibrate. The fluorescence emission spectra were then measured at 298, 304, 310, and 315 K in the wavelength range of 280−450 nm with an excitation wavelength at 250 nm. Appropriate blanks corresponding to the buffer solution were subtracted to correct background fluorescence.

To eliminate the possibility of reabsorption and inner filter effect arising from UV absorption, the fluorescence data were corrected for absorption of excitation light and emitted light according to the relationship[26]

$$F_c = F_m e^{(A_1 + A_2)/2} \quad (1)$$

where F_c and F_m are the corrected and measured fluorescence, respectively. A_1 and A_2 represent the absorbance of the drug at excitation and emission wavelengths, respectively.

CD Studies. The CD spectra of DNA incubated with farrerol at molar ratios ([farrerol]/[DNA]) of 0, 1, and 2 were measured at wavelengths between 220 and 320 nm. The changes in CD spectra were monitored against a blank. The optical chamber of the CD spectrometer was deoxygenated with dry nitrogen before use and kept in a nitrogen atmosphere during experiments. Scans were accumulated and automatically averaged. All CD measurements were carried out in a pH 7.4 Tris-HCl buffer at room temperature.

Viscosity Measurements. Viscometric titrations were preformed using a viscometer, which was kept at 25 ± 0.1 °C by a constant-temperature bath. The experiments were conducted by adding appropriate amounts of farrerol into the viscometer to give a certain r (r = [farrerol]/[DNA]) value while keeping the DNA concentration constant. The flow time of the solution through the capillary was measured with an accuracy of ±0.20 s by using a digital stopwatch. The mean values of three replicated measurements were used to evaluate the average relative viscosity of the samples. The data were presented as $(\eta/\eta_0)^{1/3}$ versus the ratios of the concentration of farrerol to that of DNA,[27] where η and η_0 represent the viscosity of DNA in the presence and absence of farrerol, respectively. Viscosity values were calculated from the observed flow time of DNA containing solutions (t) and corrected for buffer solution (t_0), $\eta = (t - t_0)/t_0$.

DNA Denaturation Studies. DNA denaturation experiments were carried out by monitoring the absorption of DNA at 260 nm in the absence and presence of farrerol at various temperatures. The absorbance intensities were then plotted as a function of temperature ranging from 20 to 100 °C. The denaturation temperature (T_m) of DNA was determined as the transition midpoint.

Chemometrics: ALS. ALS is a well-known soft modeling algorithm, which has been applied to resolve multicomponent mixtures into a simple model consisting of a composition-weighted sum of the signals of the pure compounds.[28] Multi-way UV−visible and fluorescence data were analyzed with ALS to evaluate concentration profiles and pure spectra of chemical components simultaneously present in the system from decomposition of a multivariate multicomponent experimental data matrix.

For the multiequilibria spectral data matrix $\boldsymbol{X}$, it is necessary to nominate the number of chemical species, N, which, when estimated correctly, will minimize the residual term, E. The estimation of N is commonly facilitated by any number of methods such as singular value decomposition (SVD),[29] evolving factor analysis (EFA),[30] or pure-variable detection methods, for exampe, SIMPLISMA.[31] The rank of $\boldsymbol{X}$ calculated by

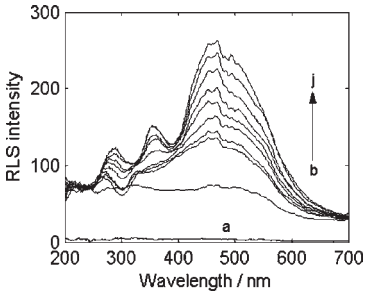

Figure 2. RLS spectra of DNA−farrerol system at pH 7.4 and room temperature. Curves: (a) c(farrerol) = 0 and c(DNA) = 7.1 × 10^{-6} mol L^{-1}; c(DNA) = 0, 0.71, 1.41, 2.11, 2.81, 3.50, 4.19, 4.87, and 5.56 × 10^{-5} mol L^{-1} for curves b−j, respectively, and c(farrerol) = 5.1 × 10^{-5} mol L^{-1}.

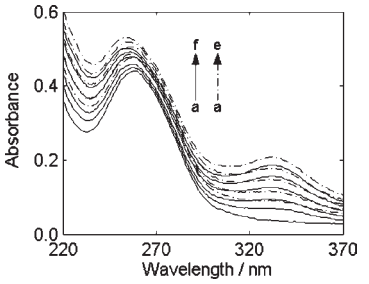

Figure 3. UV absorption spectra of DNA varying with concentrations of farrerol at pH 7.4 and room temperature. c(DNA) = 6.65 × 10^{-5} mol L^{-1}, and c(farrerol) = 0, 0.23, 0.45, 0.67, 0.89, and 1.11 × 10^{-5} mol L^{-1} for curves a−f, respectively. Solid line, measured; dashed line, theoretically summed.

any of these methods is assumed to be the number of chemical species, N, in the system. In this work, SVD was applied for this task.

The ALS process is started by initializing the concentration profiles or individual spectra, which leads to a constrained ALS optimization and eventually extracts the correct set of concentration profiles and pure individual spectral responses. This extraction process is based on the assumption that the instrumental responses of the chemical species are bilinear and can be expressed by the equation

$$\boldsymbol{X} = \boldsymbol{C}\boldsymbol{S}^{\mathrm{T}} + \boldsymbol{E} \tag{2}$$

where $\boldsymbol{X}$ is the data matrix with NR (number of spectra) rows and NC (number of wavelengths) columns, C is the NR × N dimensional concentration matrix, S^{T} is the N × NC dimensional pure spectral matrix, and $\boldsymbol{E}$ is the residual matrix, which contains the residuals.

Once the value of N is available, the initial estimation of the individual spectrum is obtained by the application of the EFA method. Then, the ALS algorithm is performed to calculate the component matrix describing the data ($\boldsymbol{C}$ and S^{T} in eq 2) by repeatedly alternating between the following two calculations until convergence. For example, if S is the initial estimation used to start the iterative process, in the first step, an estimation of the concentrations C is obtained by least-squares regression as

$$\boldsymbol{C} = X(S^{\mathrm{T}}S)^{-1} \tag{3}$$

In the second step, this new estimation of the $\boldsymbol{C}$ matrix can then be used to recalculate by least-squares (LS) a new estimation of the species spectra, S:

$$S = X^{\mathrm{T}}\boldsymbol{C}(\boldsymbol{C}^{\mathrm{T}}\boldsymbol{C})^{-1} \tag{4}$$

The LS solutions so obtained are purely mathematical and may not be appropriate from the chemical perspective; for example, they may have negative concentrations, and the spectral shapes may be unreasonable. Thus, each time eqs 3 and 4 are applied, they are submitted to constraints that require compliance with (i) all negative values of concentrations and spectra are discarded, (ii) unimodality, (iii) selectivity, and (iv) closure.[32]

RESULTS AND DISCUSSION

RLS Analysis of DNA−Farrerol Complex. Figure 2 displays the RLS spectra of DNA, farrerol, and the DNA−farrerol complex in Tris-HCl buffer (pH 7.4), respectively. From Figure 2, a remarkably enhanced RLS was observed upon addition of a trace amount of DNA to the farrerol solution, which suggested that binding between farrerol and DNA had occurred. On the basis of the theory of resonance light scattering,[33,34] it can be concluded that RLS intensity is related to the size of the formed particle and directly proportional to the square of molecular volume, and Liu et al. have demonstrated that larger particles would lead to stronger light scattering signals.[35] Therefore, after a trace amount of DNA was incorporated, a DNA−farrerol complex formed, resulting in an increase in RLS intensity.

Absorption Spectra of Interaction between Farrerol and DNA. The application of absorption spectroscopy is one of the most useful techniques in DNA-binding studies.[36] Because of compound binding to DNA, the absorbance spectrum shows hypochromism and hyperchromism, which involve a strong stacking interaction between an aromatic chromophore and the base pairs of DNA. As shown in Figure 3, the absorption peak of DNA at 260 nm exhibited gradual increase and slight blue shift with the increasing concentration of farrerol (solid line). These spectra were compared with those calculated from the sum of absorbance of free farrerol and the free DNA at their different concentrations (dashed lines). If Beer's law was strictly followed, this simulated set of spectra and the measured ones should coincide. The results showed that measured spectra (solid line) were weaker than the simulated spectra (dashed line). This hypochromic effect on the spectra of DNA−farrerol mixtures, as well as the noted slight blue spectral shift, suggested that a binary complex has formed and may be attributed to the intercalation as well as the charge attraction of farrerol to DNA bases.[37] On the basis of variations in the absorption spectra of DNA upon binding to farrerol, eq 5[38] can be utilized to calculate the binding constant, K

$$\frac{A_0}{A - A_0} = \frac{\varepsilon_{\mathrm{G}}}{\varepsilon_{\mathrm{H-G}} - \varepsilon_{\mathrm{G}}} + \frac{\varepsilon_{\mathrm{G}}}{\varepsilon_{\mathrm{H-G}} - \varepsilon_{\mathrm{G}}} \times \frac{1}{K[farrerol]} \tag{5}$$

where A_0 and A represent the absorbance of DNA in the absence and presence of farrerol and ε_{G} and $\varepsilon_{\mathrm{H-G}}$ are the absorption coefficients of the drug and its complex with DNA, respectively. The plot of $A_0/(A - A_0)$ versus 1/[farrerol] was constructed by using the absorption titration data and linear fitting, yielding the binding constant, K = 4.53 × 10^4 L mol^{-1}.

Absorption Spectra of NR Interaction with DNA. NR is a planar phenazine dye and is structurally similar to other planar dyes, for example, those of the acridine, thiazine, and xanthene kind. It has been demonstrated that the binding of NR with DNA is an intercalation binding in recent years.[22,39] Therefore, NR was employed as a spectral probe to investigate the binding mode of farrerol with DNA in the present work.

The absorption spectra of the NR dye upon addition of DNA are shown in Figure 4A. It is apparent from Figure 4A that the absorption peak of the NR at around 462 nm showed gradual

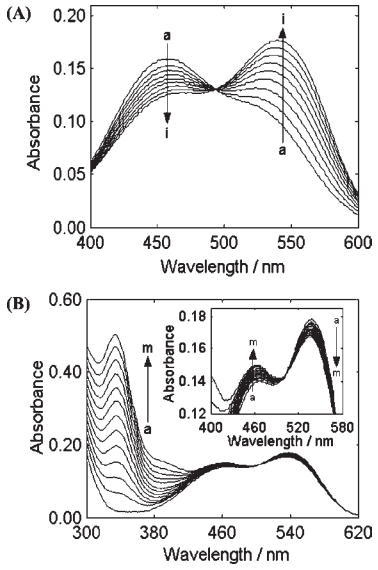

Figure 4. (A) Absorption spectra of neutral red in the presence of DNA at pH 7.4 and room temperature. c(NR) = 2.0 × 10^{-5} mol L^{-1}, and c(DNA) = 0, 0.71, 1.41, 2.11, 2.81, 3.50, 4.19, 4.87, and 5.56 × 10^{-5} mol L^{-1} for curves a−i, respectively. (B) Absorption spectra of the competitive reaction between farrerol and neutral red with DNA. c(DNA) = 6.0 × 10^{-5} mol L^{-1}, c(NR) = 2.0 × 10^{-5} mol L^{-1}, and c(farrerol) = 0, 0.23, 0.45, 0.67, 0.89, 1.11, 1.33, 1.55, 1.77, 1.98, 2.19, 2.41, and 2.62 × 10^{-5} mol L^{-1} for curves a−m, respectively. (Inset) Absorption spectra of the system with the increasing concentration of farrerol in the wavelength range of 400−580 nm.

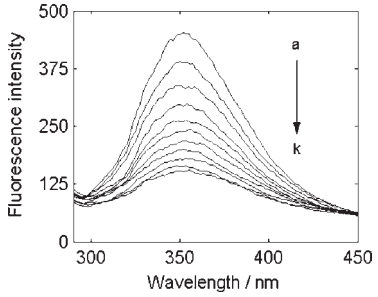

Figure 5. Fluorescence spectra of farrerol in the presence of DNA at different concentrations (pH 7.4, T = 298 K, λ_{ex} = 250 nm, λ_{em} =352 nm). c(farrerol) = 5.1 × 10^{-5} mol L^{-1}, and c(DNA) = 0, 0.71, 1.41, 2.11, 2.81, 3.50, 4.19, 4.87, 5.56, 6.23, and 6.91 × 10^{-5} mol L^{-1} for curves a−k, respectively.

decrease with the increasing concentration of DNA, and a new band at around 538 nm developed. This was attributed to the formation of the new DNA−NR complex. An isosbestic point at 503 nm provided evidence of DNA−NR complex formation.[22]

Absorption Spectra of Competitive Interaction of Farrerol and NR with DNA. Figure 4B displays the absorption spectra of a competitive binding between NR and farrerol with DNA. As shown in Figure 4B, with increasing concentration of farrerol, the maximum absorption around 538 nm of the DNA−NR complex decreased, but a slight intensity increase was observed in the developing band around 462 nm. Compared with the absorption band at around 462 nm of the free NR in the presence of increasing concentrations of DNA (Figure 4A), the spectra in Figure 4B (inset) exhibited the reverse process. The results

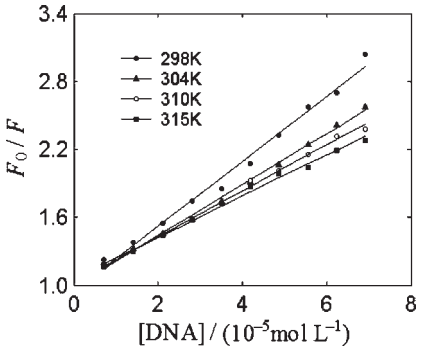

Figure 6. Stern−Volmer plots for the fluorescence quenching of farrerol by DNA at different temperatures.

suggested that farrerol intercalated into the double helix of DNA by substituting for NR in the DNA−NR complex.

Measurement of Fluorescence Spectra. At the excitation wavelength of 250 nm, the fluorescence quenching spectra of farrerol with growing amounts of DNA are shown in Figure 5. The fluorescence intensity of farrerol at around 352 nm regularly decreased, but the maximum emission wavelength of farrerol did not apparently shift with the increase of DNA concentration. The results indicated that DNA could quench the intrinsic fluorescence of farrerol and the binding of farrerol to DNA indeed exists.

It is well-known that there are two quenching processes: dynamic and static quenching. Dynamic quenching refers to a process by which the fluorophore and the quencher come into contact during the transient existence of the excited state, whereas static quenching refers to fluorophore−quencher complex formation. Static and dynamic quenching can be distinguished by their different binding constants dependent on temperature and viscosity or, preferably, by lifetime measurements.[40] In this work, we have used the binding constants dependent on the temperature to elucidate the quenching mechanism.

The fluorescence quenching data are analyzed by the Stern−Volmer eq (eq 6)[41]

$$\frac{F_0}{F} = 1 + K_{SV}[\mathrm{Q}] \tag{6}$$

where F_0 and F are the fluorescence intensities of farrerol in the absence and presence of the quencher, respectively. K_{SV} is the Stern−Volmer dynamic quenching constant. The Stern−Volmer equation was applied to determine K_{SV} by linear regression of a plot of F_0/F against [Q].

The Stern−Volmer quenching constant, K_{SV}, was observed to decrease linearly with increasing temperatures (Figure 6). These slopes (K_{SV}) were found to be (2.86 ± 0.011) × 10^4, (2.25 ± 0.005) × 10^4, (2.02 ± 0.004) × 10^4, and (1.82 ± 0.005) × 10^4 L mol^{-1} at 298, 304, 310, and 315 K, respectively, at pH 7.4. Thus, the fluorescence quenching mechanism of farrerol interaction with DNA was revealed to be not the result of dynamic collision quenching, but the consequence of static quenching.

Therefore, the fluorescence quenching of farrerol by DNA should be analyzed using the modified Stern−Volmer equation[42]

$$\frac{F_0}{F_0 - F} = \frac{1}{f_a K_a}\frac{1}{[\mathrm{Q}]} + \frac{1}{f_a} \tag{7}$$

where K_a is the modified Stern−Volmer association constant for the accessible fluorophores and f_a is the fraction of accessible fluorescence. The dependence of $F_0/(F_0-F)$ on the reciprocal

dx.doi.org/10.1021/jf2019006 |J. Agric. Food Chem. 2011, 59, 8944–8952

Table 1. Modified Stern−Volmer Association Constants and Thermodynamic Parameters for DNA−Farrerol System at Different Temperatures

T (K)	K_a ($\times 10^4$ L mol^{-1})	R^a	ΔH° (kJ mol^{-1})	ΔG° (kJ mol^{-1})	ΔS° (J K^{-1} mol^{-1})	R^b
298	3.82 ± 0.010	0.9935	−16.49 ± 0.51	−26.16 ± 0.81	32.47 ± 1.02	0.9990
304	3.40 ± 0.004	0.9928		−26.36 ± 0.82		
310	2.98 ± 0.006	0.9976		−26.56 ± 0.83		
315	2.67 ± 0.010	0.9994		−26.71 ± 0.83		

[a] R is the correlation coefficient for the K_a values. [b] R is the correlation coefficient for the van't Hoff plot.

value of the quencher concentration $1/[Q]$ is linear, with a slope equal to the value of $1/f_aK_a$. The value of $1/f_a$ is fixed on the ordinate. The constant K_a is the quotient of an ordinate $1/f_a$ and slope $1/f_aK_a$. The corresponding values of K_a at four different temperatures are summarized in Table 1. The decreasing trend of K_a with increasing temperature is in accordance with K_{SV}'s dependence on temperature as discussed above, a characteristic that accords with the type of static quenching. The value of K_a at 298 K is 3.82 × 10^4 L mol^{-1}, which agrees with the value obtained earlier by UV spectroscopy and supports the effective role of static quenching.[43]

Thermodynamic Analysis and the Nature of the Binding Forces. The interaction forces between small molecules and biomolecules mainly include hydrogen bonds, van der Waals force, hydrophobic force, and electrostatic interactions. The thermodynamic parameters of binding reaction are the main evidence for confirming the binding force. If the enthalpy change (ΔH°) does not vary significantly over the temperature range studied, then its value and that of entropy change (ΔS°) can be determined from the van't Hoff equation:[44]

$$\log K_a = -\frac{\Delta H^\circ}{2.303RT} + \frac{\Delta S^\circ}{2.303R} \quad (8)$$

In eq 8, R is the gas constant. The temperatures used were 298, 304, 310, and 315 K. The values of ΔH° and ΔS° were obtained from the slope and intercept of the linear van't Hoff plot based on log K_a versus $1/T$. The free energy change (ΔG°) was then evaluated from the following equation:[45]

$$\Delta G^\circ = \Delta H^\circ - T\Delta S^\circ \quad (9)$$

Table 1 lists the thermodynamic parameters for the interaction of farrerol with DNA. The negative values of ΔG° revealed that the binding process is spontaneous. The positive value of ΔS° is frequently regarded as evidence for a hydrophobic interaction.[46,47] The negative ΔH° value showed that the binding process is mainly enthalpy driven and by means of hydrogen binding interactions.[48] Thus, both hydrophobic interactions and hydrogen bonds play a major role in the binding of farrerol to DNA and contribute to the stability of the complex.

Iodide Quenching Studies. A highly negatively charged quencher is expected to be repelled by the negatively charged phosphate backbone of DNA. Therefore, if the binding mode of a small molecule with DNA is intercalation, the molecule should be protected from being quenched by anionic quencher. Different from intercalation, groove binding provides much less protection for the bound molecule.[49] The value of quenching constants (K_{SV}) of the intercalative bound molecule should be lower than that of the molecule bound to DNA by groove binding. Negatively charged I^- was selected for this purpose. The values of K_{SV} of farrerol by I^- ion in the absence and presence of DNA were calculated to be 6.22 × 10^3 and 4.96 × 10^3 L mol^{-1}, respectively, by the Stern−Volmer equation (Figure 7). The results showed that iodide quenching effect was decreased when farrerol was bound to DNA, suggesting that the binding mode of farrerol with DNA is of intercalation nature.

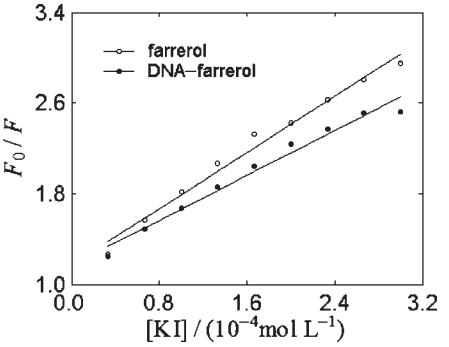

Figure 7. Fluorescence quenching plots of farrerol by KI in the absence and presence of DNA at pH 7.4 and room temperature. c(farrerol) = 5.1 × 10^{-5} mol L^{-1}, and c(DNA) = 2.13 × 10^{-5} mol L^{-1}.

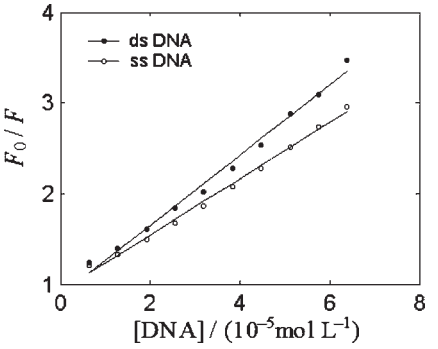

Figure 8. Fluorescence quenching plots of farrerol by dsDNA and ssDNA at pH 7.4 and room temperature. c(farrerol) = 5.1 × 10^{-5} mol L^{-1}, and c(DNA) = 2.13 × 10^{-5} mol L^{-1}.

Comparison of the Interactions of Farrerol with Single-Stranded and Double-Stranded DNA. Further support for the intercalative binding of farrerol to DNA was obtained through the fluorescence quenching effect of both single-stranded DNA (ssDNA) and double-stranded DNA (dsDNA) on farrerol. The ssDNA solution was prepared by heating native dsDNA solution in a boiling water bath for 10 min and then cooling rapidly in an ice−water bath. If there was electrostatic interaction, the quenching effect on the drug and dsDNA should be the same (interact with phosphate groups). If there was a groove binding, the quenching effect on the drug should be strengthened compared to dsDNA. If there was an intercalating mode, the quenching effect on the drug would be reduced compared to dsDNA (the

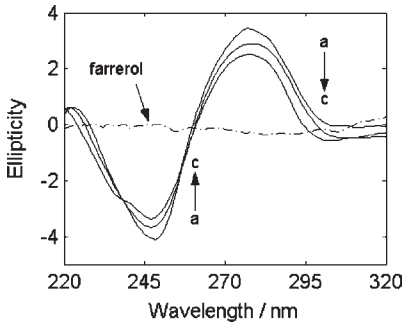

Figure 9. Circular dichroism spectra of DNA in the presence of increasing amounts of farrerol (r_i = [farrerol]/[DNA]) at pH 7.4 and room temperature. c(farrerol) = 4.0 × 10^{-4} mol L^{-1} (dashed line), and c(DNA) = 4.0 × 10^{-4} mol L^{-1}. The values of r_i were 0 (a), 1(b), and 2 (c), respectively.

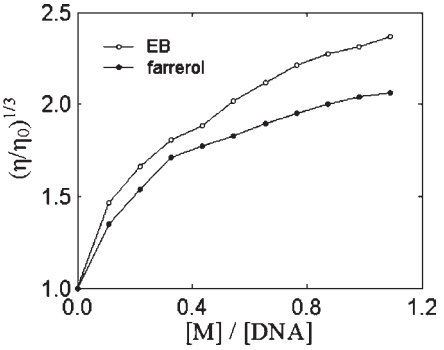

Figure 10. Effect of increasing amounts of farrerol and ethidium bromide (EB) on the relative viscosity of DNA at 298 K. c(DNA) = 2.13 × 10^{-5} mol L^{-1}; pH 7.4.

double-helix structure of dsDNA was damaged in the preparation of ssDNA).[50] As can be seen from Figure 8, the quenching effect on the fluorescence of farrerol would be reduced when ssDNA was compared with dsDNA, which revealed further that that the binding mode of farrerol to DNA is intercalation.

CD Studies. The changes in CD signals of DNA observed on interaction with small molecules may be assigned to the corresponding changes in DNA structure, as a positive band at 275 nm due to base stacking and a negative band at 246 nm due to right-handed helicity are quite sensitive to the mode of DNA interactions with small molecules.[51] Groove binding and electrostatic interaction of small molecules show less or no perturbation on the base stacking and helicity bands, whereas intercalation changes the intensities of both bands, thus stabilizing the right-handed B conformation of DNA.[52] CD spectra of DNA−farrerol systems are shown in Figure 9. It can be seen from Figure 9 that the intensities of the negative band decreased significantly (shifting to zero levels) accompanied by a slight blue shift at about 4.0 nm, whereas the positive band decreased without any significant shift with increasing [farrerol]/[DNA] ratio. This revealed the effect of intercalation of farrerol in base stacking and decreased right-handedness of the DNA.[53,54]

Viscosity Measurements. Viscosity experiments are an effective tool to detect binding modes between small molecules and DNA. Generally, a classical intercalation binding causes an increase in the viscosity of DNA solution because it demands a large enough space of adjacent base pairs to accommodate the

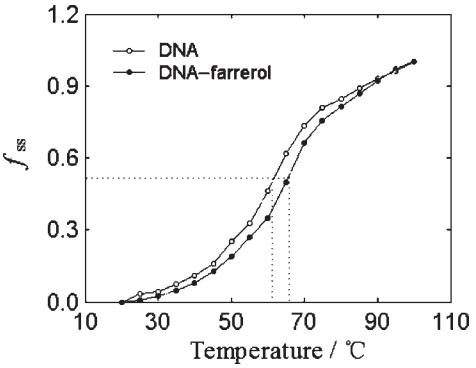

Figure 11. Melting curves of DNA in the absence and presence of farrerol at pH 7.4. c(farrerol) = 5.1 × 10^{-5} mol L^{-1}, and c(DNA) = 2.13 × 10^{-5} mol L^{-1}.

ligand and to lengthen the double helix.[55] In contrast, there is little effect on the viscosity of DNA if electrostatic or groove binding occurs in the binding process.[56] Figure 10 exhibits the changes of relative viscosity of DNA in the presence of various concentrations of farrerol. It can be observed from Figure 10 that the viscosity of DNA remarkably increased upon the addition of farrerol, which is very similar to the increasing trend of DNA viscosity with increasing concentration of ethidium bromide (EB), a typical DNA intercalator. The results provide strong evidence for intercalative binding of farrerol with DNA.

DNA Denaturation Temperature Studies. The DNA melting study is further evidence for the intercalation of farrerol into the DNA helix. The denaturation temperature (T_m) of DNA at which half of a DNA sample is melted is sensitive to its double-helix stability, and the binding of compounds to DNA alters the T_m depending on the strength of interactions. It is well documented that the intercalation of natural or synthetic compounds into DNA generally results in T_m increases of about 5−8 °C, but the nonintercalation binding causes no obvious increase in T_m.[47] The change in absorbance at 260 nm for the DNA in the absence and presence of farrerol was measured. The values of T_m of DNA and the DNA−farrerol system were obtained from the transition midpoint of the melting curves based on f_{ss} versus temperature (T), where $f_{ss} = (A - A_0)/(A_f - A_0)$, where A_0 is the initial absorbance intensity, A is the absorbance intensity corresponding to its temperature, and A_f is the final absorbance intensity.[57] The melting curves of DNA in the absence and presence of farrerol are shown in Figure 11. It can be seen that the T_m of DNA in the absence of farrerol is 60.4 °C, whereas T_m of DNA in the presence of farrerol is 65.5 °C. The interaction of farrerol with DNA can cause the denaturation temperature to be increased, which indicated that the stabilization of the DNA helix was increased in the presence of farrerol. This stabilizing action of farrerol is very similar to that observed previously with chlorobenzylidine[58] and Pt(II) complex.[59] This provides further support for the intercalation of farrerol into the dsDNA helix.

Application of ALS for the Resolution of the Two-Dimensional UV−Vis Spectra. Generally, for the UV−vis spectra alone (Figure 4B), it is difficult to deduce the formation of a complex in the competitive binding reaction system because of the high spectral overlap for each species. Hence, in the present work the spectroscopic data matrix was resolved by the ALS algorithm to obtain useful information of the binding reaction system,

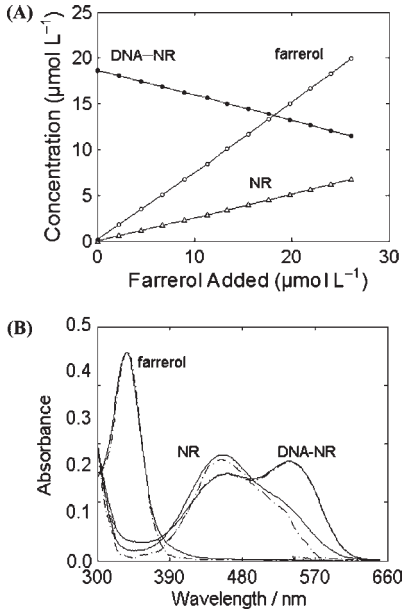

Figure 12. (A) Equilibrium concentrations of farrerol, NR, and DNA–NR complex extracted by the ALS chemometrics method. The farrerol was present at different concentrations. The conditions are as in Figure 4. (B) Comparison of the measured absorption spectra for farrerol, NR, and DNA–NR complex with those obtained from ALS modeling. Solid line, resolved spectra from ALS; dashed line, measured spectra.

including the DNA–NR complex, the concentration profiles, and the pure spectra for each species.

To apply the ALS algorithm, the first step was to evaluate the number of factors that could be related to chemical species by the SVD model. The next step was to estimate the concentration and to extract the corresponding pure spectra for the species existing in the binding procedure.

The ALS algorithm was applied to investigate the competitive binding interactions between farrerol and NR with DNA. The absorption data matrix was processed with the aid of the SVD model, and the extracted seven eigenvalues were 12.5736, 2.3378, 0.5322, 0.0125, 0.0081, 0.0073, and 0.0066, indicating that there were arguably three significant factors for prediction of the three separate chemical components in the system, that is, farrerol, NR, and DNA–NR complex; however, as noted previously, the spectra of these three substances in mixtures overlapped considerably. The estimation of concentrations of each component at equilibrium during the titration process was not possible by conventional methods. Therefore, the ALS method was applied to resolve the two-way UV–vis spectra (Figure 4B).

It can be seen from Figure 12B that the resolved spectra (solid line) of the three reaction components (farrerol, NR, and DNA–NR) compared well with their measured counterparts (dashed line). This suggested that the results of the ALS model were unique and reliable and that the correct number of components for the model was chosen. As shown from Figure 12A, the increasing addition of farrerol resulted in a decrease in the concentration of the DNA–NR complex and an increase in the concentration of free NR. The displacement of NR in the DNA–NR complex by farrerol can be visualized clearly, indicating that farrerol intercalates into the same base sites of DNA, releasing the bound NR. The ALS analysis further verified the above results obtained by other methods.

In conclusion, the binding interactions of farrerol with calf thymus DNA have been studied using UV–vis absorption, fluorescence, and CD spectroscopy. The results indicated that the binding mode of farrerol to DNA is an intercalation binding, which was supported by the results from DNA melting studies and viscosity measurements. Furthermore, ALS modeling was used to resolve the absorption data matrix of the competitive reaction between farrerol and NR with DNA, which provided simultaneously concentration information and the corresponding pure spectra for the three reaction components, farrerol, NR, and DNA–NR complex, in the system at equilibrium. This clearly indicated the intercalation of the farrerol molecule into the DNA by substituting for NR probe in the DNA–NR complex. Moreover, the association constants and thermodynamic parameters of farrerol with DNA were calculated. It was found that both hydrophobic interactions and hydrogen bonds play a major role in the binding of farrerol to DNA.

Studies show that flavonoids can bind DNA by intercalation and that the planarity of the chromophore is a limiting factor in the interaction.[60] Recently, Sun et al.[61] investigated the binding of the flavonoids baicalein, wogonin, and baicalin to DNA by absorption, fluorescence, melting temperature, and viscosity measurements. The binding constants of the flavonoids with DNA were 5.30×10^4, 1.33×10^5, and 2.40×10^4 L mol^{-1} at 298 K, respectively. Their studies indicated that these flavonoids intercalated into the dsDNA helix, which accounts for the high binding constant. Their experimental results are similar to those of our present study, which might be attributed to the similar chemical structures of the flavonoids.

AUTHOR INFORMATION

Corresponding Author

*Phone: +867918305234. Fax: +867918304347. E-mail: gwzhang@ncu.edu.cn.

Funding Sources

We gratefully acknowledge the financial support of the National Natural Science Foundation of China (No. 31060210), the Program of Science and Technology of Jiangxi Province (2009BNA09000, 2010BSA17400), the Natural Science Foundation of Jiangxi Province (2009GZH0069), the Research Program of State Key Laboratory of Food Science and Technology of Nanchang University (SKLF-TS-200917, SKLF-MB-201002), and the Foundation of Jiangxi Provincial Office of Education (GJJ11287).

REFERENCES

(1) Sahoo, B. K.; Ghosh, K. S.; Bera, R.; Dasgupta, S. Study on the interaction of diacetylcurcumin with calf thymus-DNA. *Chem. Phys.* **2008**, *351*, 163–169.

(2) Yola, M. L.; Özaltın, N. Electrochemical studies on the interaction of an antibacterial drug nitrofurantoin with DNA. *J. Electroanal. Chem.* **2011**, *653*, 56–60.

(3) Zhang, Y.; Wang, X. M.; Ding, L. S. Interaction between tryptophan–vanillin Schiff base and herring sperm DNA. *J. Serb. Chem. Soc.* **2010**, *75*, 1191–1201.

(4) Tan, J.; Wang, B. C.; Zhu, L. C. DNA binding, cytotoxicity, apoptotic inducing activity, and molecular modeling study of quercetin–zinc(II) complex. *Bioorg. Med. Chem.* **2009**, *17*, 614–620.

(5) Andarwulan, N.; Batari, R.; Sandrasari, D. A.; Bolling, B.; Wijaya, H. Flavonoid content and antioxidant activity of vegetables from Indonesia. *Food Chem.* **2010**, *121*, 1231–1235.

(6) Leopoldini, M.; Russo, N.; Toscano, M. A comparative study of the antioxidant power of flavonoid catechin and its planar analogue. *J. Agric. Food Chem.* **2007**, *55*, 7944–7949.

(7) Tian, J. N.; Liu, J. Q.; Hu, Z. D.; Chen, X. G. Interaction of wogonin with bovine serum albumin. *Bioorg. Med. Chem.* **2005**, *13*, 4124–4129.

(8) Papadopoulou, A.; Green, R. J.; Frazier, R. A. Interaction of flavonoids with bovine serum albumin: a fluorescence quenching study. *J. Agric. Food Chem.* **2005**, *53*, 158–163.

(9) Vitorino, J.; Sottomayor, M. J. DNA interaction with flavone and hydroxyflavones. *J. Mol. Struct.* **2010**, *975*, 292–297.

(10) Ji, Y. B. *Pharmacology and Applied of Effective Ingredient from Chinese Traditional Medicine*; Science Press of Heilongjiang: Harbin, China, 1994; pp 261−263

(11) Jin, J.; Zhu, J. F.; Yao, X. J.; Wu, L. M. Study on the binding of farrerol to human serum albumin. *J. Photochem. Photobiol. A: Chem.* **2007**, *191*, 59–65.

(12) Li, D. J; Wang, Y.; Chen, J. J.; Ji, B. M. Characterization of the interaction between farrerol and bovine serum albumin by fluorescence and circular dichroism. *Spectrochim. Acta A* **2011**, *79*, 680–686.

(13) Shi, L.; Feng, X. E.; Cui, J. R.; Fang, L. H.; Du, G. H.; Li, Q. S. Synthesis and biological activity of flavanone derivatives. *Bioorg. Med. Chem. Lett.* **2010**, *20*, 5466–5468.

(14) Akbay, N.; Seferoglu, Z.; Gokoglu, E. Interactions of two ethidium derivatives with calf thymus DNA and serum albumins using fluorescence quenching method. *Curr. Anal. Chem.* **2010**, *4*, 334–340.

(15) Janjua, N. K.; Siddiqa, A.; Yaqub, A.; Sabahat, S.; Qureshi, R.; Haque, S. U. Spectrophotometric analysis of flavonoid−DNA binding interactions at physiological conditions. *Spectrochim. Acta A* **2009**, *74*, 1135–1137.

(16) Kalanur, S. S.; Katrahalli, U.; Seetharamappa, J. Electrochemical studies and spectroscopic investigations on the interaction of an anticancer drug with DNA and their analytical applications. *J. Electroanal. Chem.* **2009**, *636*, 93–100.

(17) Jangir, D. K.; Tyagi, G.; Mehrotra, R.; Kundu, S. Carboplatin interaction with calf-thymus DNA: A FTIR spectroscopic approach. *J. Mol. Struct.* **2010**, *969*, 126–129.

(18) Bocian, W.; Kawęcki, R.; Bednarek, E.; Sitkowski, J.; Ulkowska, A.; Kozerski, L. Interaction of flavonoid topoisomerase I and II inhibitors with DNA oligomers. *New J. Chem.* **2006**, *30*, 467–472.

(19) Liu, Y. Q.; Li, H. H.; Ye, Y. H.; Yuan, G. Investigation of the interaction between HIV-1 DNA and cyclic peptides by electrospray ionization mass spectrometry. *Chin. Chem. Lett.* **2009**, *20*, 330–333.

(20) Mendieta, J.; Díaz-Cruz, M. S.; Tauler, R.; Esteban, M. Application of multivariate curve resolution to voltammetric data. *Anal. Biochem.* **1996**, *240*, 134–141.

(21) Diaz-Cruz, J. M.; Tauler, R.; Grabaric, B. S.; Esteban, M.; Casassas, E. Application of multivariate curve resolution to voltammetric data. Part 1. Study of Zn(II) complexation with some polyelectrolytes. *J. Electroanal. Chem.* **1995**, *393*, 7–16.

(22) Ni, Y. N.; Du, S.; Kokot, S. Interaction between quercetin−copper(II) complex and DNA with the use of the Neutral Red dye fluorophor probe. *Anal. Chim. Acta* **2007**, *584*, 19–27.

(23) Zhang, G. W.; Guo, J. B.; Zhao, N.; Wang, J. R. Study of interaction between kaempferol−Eu^{3+} complex and DNA with the use of the Neutral Red dye as a fluorescence probe. *Sens. Actuat. B* **2010**, *144*, 239–246.

(24) Kanakis, C. D.; Nafisi, Sh.; Rajabi, M.; Shadaloi, A.; Tarantilis, P. A.; Polissiou, M. G.; Bariyanga, J.; Tajmir-Riahi, H. A. Structural analysis of DNA and RNA interactions with antioxidant flavonoids. *Spectroscopy* **2009**, *23*, 29–43.

(25) Mahadevan, S.; Palaniandavar, M. Spectroscopic and voltammetric studies on copper complexes of 2,9-dimethyl-1,10-phenanthrolines bound to calf thymus DNA. *Inorg. Chem.* **1998**, *37*, 693–700.

(26) Steiner, R. F.; Weinryb, L. *Excited States of Protein and Nucleic Acid*; Plenum Press: New York, 1971; p 40.

(27) Zhao, N.; Wang, X. M.; Pan, H. Z.; Hu, Y. M.; Ding, L. S. Spectroscopic studies on the interaction between tryptophan−erbium(III) complex and herring sperm DNA. *Spectrochim. Acta A* **2010**, *75*, 1435–1442.

(28) Tauler, R. Multivariate curve resolution applied to second order data. *Chemom. Intell. Lab. Syst.* **1995**, *30*, 133–146.

(29) Malinowski, E. R. *Factor Analysis in Chemistry*, 3rd ed.; Wiley: New York, 2002.

(30) Maeder, M. Evolving factor analysis for the resolution of overlapping chromatographic peaks. *Anal. Chem.* **1987**, *59*, 527–530.

(31) Windig, W.; Guilment, J. Interactive self-modeling mixture analysis. *Anal. Chem.* **1991**, *63*, 1425–1432.

(32) Tauler, R.; Casassas, E.; Izquierdo-Ridorsa, A. Self-modelling curve resolution in studies of spectrometric titrations of multi-equilibria systems by factor analysis. *Anal. Chim. Acta* **1991**, *248*, 447–458.

(33) Yang, J.; Chen, X. D.; Fu, R. W.; Luo, W. A.; Li, Y. B.; Zhang, M. Q. Kinetics of phase separation in polymer blends revealed by resonance light scattering spectroscopy. *Phys. Chem. Chem. Phys.* **2010**, *12*, 2238–2245.

(34) Zhang, G. W.; Chen, X. X; Guo, J. B.; Wang, J. J. Spectroscopic investigation of the interaction between chrysin and bovine serum albumin. *J. Mol. Struct.* **2009**, *921*, 346–351.

(35) He, Y. Q.; Liu, S. P.; Kong, L.; Liu, Z. F. A study on the sizes and concentrations of gold nanoparticles by spectra of absorption, resonance Rayleigh scattering and resonance non−linear scattering. *Spectrochim. Acta A* **2005**, *61*, 2861–2866.

(36) Tong, C. L.; Xiang, G. H.; Bai, Y. Interaction of paraquat with calf thymus DNA: a terbium(III) luminescent probe and multispectral study. *J. Agric. Food Chem.* **2010**, *58*, 5257–5262.

(37) Ni, Y. N.; Lin, D. Q.; Kokot, S. Synchronous fluorescence, UV−visible spectrophotometric, and voltammetric studies of the competitive interaction of bis(1,10-phenanthroline) copper(II) complex and neutral red with DNA. *Anal. Biochem.* **2006**, *352*, 231–242.

(38) Devi, C. V.; Singh, N. R. Absorption spectroscopic probe to investigate the interaction between Nd(III) and calf-thymus DNA. *Spectrochim. Acta A* **2011**, *78*, 1180–1186.

(39) Wang, Y. T.; Zhao, F. L.; Li, K. A.; Tong, S. Y. Molecular spectroscopic study of DNA binding with neutral red and application to assay of nucleic acids. *Anal. Chim. Acta* **1999**, *396*, 75–81.

(40) Xu, J. G.; Wang, Z. B. *Methods of Fluorescence Analysis*, 3rd ed., Science Press: Beijing, China, 2006; pp 64−85.

(41) Lakowicz, J. R. *Principles of Fluorescence Spectroscopy*, 3rd ed.; Springer Publications,: New York, 2006.

(42) Yang, M. M.; Xi, X. L.; Yang, P. Study of the interaction of cephalosporin class medicine with albumin by fluorescence enhancement and fluorescence quenching theories. *Chin. J. Chem.* **2006**, *24*, 642–648.

(43) Darwish, S. M.; Sharkh, S. E. A.; Teir, M. M. A.; Makharza, S. A.; Abu-hadid, M. M. Spectroscopic investigations of pentobarbital interaction with human serum albumin. *J. Mol. Struct.* **2010**, *963*, 122–129.

(44) Zhao, N.; Wang, X. M.; Pan, H. Z.; Hu, Y. M.; Ding, L. S. Spectroscopic studies on the interaction between tryptophan−erbium(III) complex and herring sperm DNA. *Spectrochim. Acta A* **2010**, *75*, 1435–1442.

(45) Ortiz, M.; Fragosoa, A.; Ortiz, P. J.; O'Sullivan, C. K. Elucidation of the mechanism of single-stranded DNA interaction with methylene blue: a spectroscopic approach. *J. Photochem. Photobiol. A* **2011**, *218*, 26–32.

(46) Ross, P. D.; Subramanian, S. Thermodynamics of protein association reaction: forces contributing to stability. *Biochemistry* **1981**, *20*, 3096–3102.

(47) Bi, S. Y.; Zhang, H. Q.; Qiao, C. Y. Studies of interaction of emodin and DNA in the presence of ethidium bromide by spectroscopic method. *Spectrochim. Acta A* **2008**, *69*, 123–129.

(48) Yuan, J. L.; Liu, H.; Kang, X.; Lv, Z.; Zou, G. L. Characteristics of the isomeric flavonoids apigenin and genistein binding to hemoglobin by spectroscopic methods. *J. Mol. Struct.* **2008**, *891*, 333–339.

(49) Akbay, N.; Seferoğlu, Z.; Gök, E. Fluorescence interaction and determination of calf thymus DNA with two ethidium derivatives. *J. Fluoresc.* **2009**, *19*, 1045–1051.

(50) Cai, C. Q.; Chen, X. M.; Ge, F. Analysis of interaction between tamoxifen and ctDNA in vitro by multi-spectroscopic methods. *Spectrochim. Acta A* **2010**, *76*, 202–206.

(51) Wang, J.; Yang, Z. Y.; Yi, X. Y.; Wang, B. D. DNA-binding properties studies and spectra of a novel fluorescent Zn(II) complex with a new chromone derivative. *J. Photochem. Photobiol. A* **2009**, *201*, 183–190.

(52) Silvestri, A.; Barone, G.; Ruisi, G.; Anselmo, D.; Riela, S.; Liveri, V. T. The interaction of native DNA with Zn(II) and Cu(II) complexes of 5-triethyl ammonium methyl salicylidene ortho-phenylendiimine. *J. Inorg. Biochem.* **2007**, *101*, 841–848.

(53) Xu, X. Y.; Wang, D. D.; Sun, X. J.; Zeng, S. Y.; Li, L. W.; Sun, D. Z. Thermodynamic and spectrographic studies on the interactions of ct-DNA with 5-fluorouracil and tegafur. *Thermochim. Acta* **2009**, *493*, 30–36.

(54) Maheswari, P. U.; Palaniandavar, M. DNA binding and cleavage properties of certain tetrammine ruthenium(II) complexes of modified 1,10-phenanthrolines-effect of hydrogen-bonding on DNA-binding affinity. *J. Inorg. Biochem.* **2004**, *98*, 219–230.

(55) Kashanian, S.; Dolatabadi, J. E. N. DNA binding studies of 2-*tert*-butylhydroquinone (TBHQ) food additive. *Food Chem.* **2009**, *116*, 743–747.

(56) Bi, S. Y.; Qiao, C. Y.; Song, D. Q.; Tian, Y.; Gao, D. J.; Sun, Y.; Zhang, H. Q. Study of interactions of flavonoids with DNA using acridine orange as a fluorescence probe. *Sens. Actuat. B* **2006**, *119*, 199–208.

(57) Zhao, P.; Huang, J. W.; Mei, W. J.; He, J.; Ji, L. N. DNA binding and photocleavage specificities of a group of tricationic metalloporphyrins. *Spectrochim. Acta A* **2010**, *75*, 1108–1114.

(58) Zhong, W. Y.; Yu, J. S.; Liang, Y. Q.; Fan, K. Q.; Lai, L. H. Chlorobenzylidine−calf thymus DNA interaction II: circular dichroism and nuclear magnetic resonance studies. *Spectrochim. Acta A* **2004**, *60*, 2985–2992.

(59) Shahabadi, N.; Kashanian, S.; Purfoulad, M. DNA interaction studies of a platinum(II) complex, PtCl2(NN) (NN = 4,7-dimethyl-1,10-phenanthroline), using different instrumental methods. *Spectrochim. Acta A* **2009**, *72*, 757–761.

(60) Solimani, R.; Bayon, F.; Domini, I.; Pifferi, P. G.; Todesco, P. E.; Marconi, G.; Samori, B. Flavonoid−DNA interaction studied with flow linear dichroism technique. *J. Agric. Food Chem.* **1995**, *43*, 876–882.

(61) Sun, Y. T.; Bi, S. Y.; Song, D. Q.; Qiao, C. Y.; Mu, D.; Zhang, H. Q. Study on the interaction mechanism between DNA and the main active components in *Scutellaria baicalensis Georgi*. *Sens. Actuat. B* **2008**, *129*, 799–810.